https://doi.org/10.5194/egusphere-2026-2885
Preprint. Discussion started: 12 June 2026

Method for Consistency Analysis of a set of space-borne Climate Data Records: Application to Aerosol Optical Depth

Ulrike Stöffelmair[1], Diana Dermann[1], and Thomas Popp[1]

[1]German Remote Sensing Data Center (DFD), German Aerospace Center (DLR), 82234 Oberpfaffenhofen, Germany

Correspondence: Ulrike Stöffelmair (ulrike.stoeffelmair@dlr.de)

Abstract. The consistency of a set of satellite observations obtained with different algorithms from the same satellite instruments can be used as an indicator for their robustness or reliability. For this four metrics to evaluate those characteristics are defined and integrated into one overall consistency score per grid cell. These four metrics are: their median values, annual cycle, median values, decadal trends and correlation. This paper discusses how a combination of these metrics can be used to evaluate the overall consistency of different datasets for the same essential climate data variable.

This study performs an examplary application of this approach on Aerosol Optical Depth (AOD) Climate Data Records (CDRs) obtained from a series of 3 similar instruments from the Copernicus Climate Change Service (C3S). Assessing the consistency of those CDRs is highly relevant because space-based aerosol information and their climate impact have substantial uncertainties. The regional dependency of this consistency score shows the influence of surface properties and geographic regions. With the consistency score, regions with robust information can be separated from more challenging regions and the advantages and disadvantages of different instruments can be identified.

1 Introduction

Monitoring the climate with satellite measurements is essential for a systematic global analysis and also as input into climate models, because of the global coverage, which ground-based measurements can not provide. As satellite inversion-based datasets come with substantial uncertainties, their validation and comparison between different retrieved datasets is needed. As the validation against ground measurements is limited by the spatial distribution of stations, a systematic way to analyse the consistency of different datasets on global scale is needed. Within the ESA Climate Change Initiative (CCI) (Hollmann et al., 2013) underlying the Copernicus Climate Change Service (C3S), a comprehensive definition of "consistency" on three levels (technical, retrieval and scientific) and criteria for its evaluation have been worked out (Popp et al., 2020). This study implements a concrete realization of this concept by using a combination of four different metrics: annual cycle, median values, decadal trends and correlation.

As aerosols are the most uncertain climate change drivers according to IPCC (Intergovernmental Panel on Climate Change) (Arias et al., 2021; Allen et al., 2018), we exemplarily apply the method described in Section 2 on Aerosol Optical Depth (AOD) Climate Data Records (CDR). Satellite measurements have been used for aerosol retrieval for over four decades (Kokhanovsky

https://doi.org/10.5194/egusphere-2026-2885
Preprint. Discussion started: 12 June 2026

and Leeuw, 2009; de Leeuw et al., 2015). However, there are larger uncertainties in satellite inversions than in ground measurements (Sogacheva et al., 2020). This requires a more detailed examination of the satellite retrievals from different measuring instruments and different retrieval algorithms. The retrievals can only be considered reliable and used for further analysis of the effects of aerosols if different datasets of the same quantity deliver results which agree with each other, often expressed as meeting requirements for "consistency".

Three algorithms based on different physical principles and applying different quality control strategies Kokhanovsky and Leeuw (2009); de Leeuw et al. (2015); Flowerdew and Haigh (1995); Veefkind et al. (1998); Kolmonen et al. (2016); Sogacheva et al. (2017); North et al. (1999); North (2002); Bevan et al. (2012); Thomas et al. (2009); Sayer et al. (2010) have been developed for the retrieval of aerosol properties to optimally use the available information from the dual-view instruments (radiances measured at the top of the atmosphere at different wavelengths, in the visible and infrared, and with two different viewing angles). They are described briefly in Section 3.1. It is known from earlier analysis that none of the algorithms outperforms the others everywhere Sogacheva et al. (2020).

In this study, these three aerosol retrieval algorithms are evaluated for their suitability to produce consistent aerosol CDRs suitable for long-term monitoring. The algorithms were developed in the context of the Aerosol_cci (Popp et al., 2016) project before long-term records from European instruments were processed using them in the C3S (https://climate.copernicus.eu/) project on atmospheric composition focusing on European instruments. The data processed is exploited from three similar (but not identical!) subsequent dual-view radiometers (Along Track Scanning Radiometer 2 (ATSR-2, 1995-2003), Advanced ATSR (AATSR, 2002-2012) and Sea and Land Surface Temperature Radiometer (SLSTR, since 2016))

The aim of this study is to demonstrate the value of different consistency metrics and their combination into an overall consistency score as described in Section 2 to analyse the consistency of satellite based datasets for every grid cell on the globe, especially where no ground-based stations are available. This information shall support a user to easily obtain an overview of the suitability of an ensemble of datasets for one sensor in different regions using the appropriate metric(s) depending on the study focus of an intended application.

In Section 3.2 the individual metrics are applied exemplarily to the three datasets for each of the three instruments and finally their combined consistency score is assessed. It shows the influence of surface properties, aerosol amount, geographic region and instrument viewing direction, which are all discussed in Section 3.3. Finally, the combined analysis is used to identify regions with most reliable information in the datasets and to highlight advantages and disadvantages of the three different subsequent instruments.

In addition, in Section 4 the method is evaluated and it is discussed how the method can be adjusted for other studies depending on their focus, for example on long-term trends or seasonal variability.

https://doi.org/10.5194/egusphere-2026-2885
Preprint. Discussion started: 12 June 2026

2 Methods to analyse consistency

The developed method for analysing the consistency between different datasets is shown in the flowchart in Figure 1. We define these four metrics to objectively assess the consistency per grid cell: (A) the median value, (B) the linear trend, (C) the amplitude of the averaged annual cycle and (D) the correlation.

In the case presented here we are analysing the consistency between three datasets. They are based on the same measured data but retrieve the aerosol properties using different algorithms. This means that there are three datasets for each radiometer that can be compared. This study uses Level 3 monthly data on a 1°x1° grid.

The first three metrics are computed on the 1°x1° grid and subsequently averaged to a 5°x5° grid. The mean value and the standard deviation for each metric are calculated if more than 10 of the 25 1°x1° grid cells have a valid value. In addition, for each metric a threshold is defined which if met for a grid cell means that consistency if fulfilled. For the first three metrics, the algorithms are considered consistent, if the difference of the metric for the different algorithms is within 2 standard deviations of all three algorithms. The correlation coefficient for each pair of algorithms as a further metric for consistency is calculated directly on the 5°x5° grid. It is accepted as consistent if none of the correlation coefficients for the different algorithms combinations is smaller than 0.7.

Finally, for each fulfilled metric, 1 point is given and all points are summed up across each grid cell to obtain the total consistency score. If three or four points are reached, the grid cell is considered as (highly) consistent.

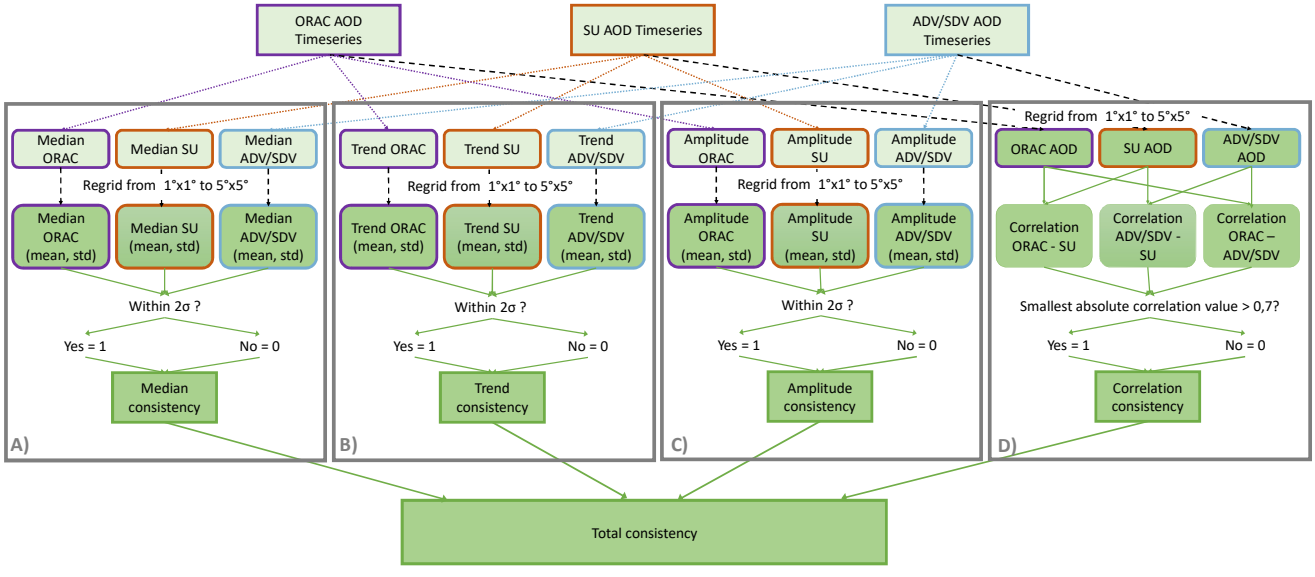

Figure 1. Flowchart of the applied method for illustration.

https://doi.org/10.5194/egusphere-2026-2885
Preprint. Discussion started: 12 June 2026

2.1 Metric A: Median values

The first metric is the median value. We use the median values of the data from each of the different algorithms to measure biases between them.

$$x_{\text{median}} = \begin{cases} x_{m+1} & \text{for odd n=2m+1} \\ 0.5(x_m + x_{m+1}) & \text{for even n=2m} \end{cases} \quad (1)$$

The median allows the outliers to be disregarded and is therefore more robust and thus better suited for analysing consistency than the mean value. No filtering of "bad" data is applied.

2.2 Metric B: Mann-Kendall trend test

Trends are calculated with a seasonal Mann-Kendall trend test using the Python package pyMannKendall (Hussain and Mahmud, 2019) from time records of monthly averages.

The Mann-Kendall test (Mann, 1945; Kendall, 1970) is a non-parametric test for determining a monotonic trend in a time series. Non-parametric tests are better suited than parametric tests for non-normally distributed, partially masked and missing data (Li et al., 2014) and are therefore used for the satellite based data considering the gaps for example created by cloud masking.

The Mann-Kendall trend test using the Theil-Sen Estimator calculates the slope of the trend as the median of the slopes of every possible connecting line between two points of the dataset $X = x_1, x_2, ..., x_n$. In order to take seasonality into account, the data is assessed on a monthly basis and then used to calculate the total expected value, the variance, the standardized test statistic Z and the overall trend b (Hirsch et al., 1982).

$$b = \text{med}\left(\frac{x_j - x_k}{j - k}\right) \quad \forall \quad 1 \leq k < j \leq n \quad (2)$$

For the consistency analysis we use all trend data calculated, except the unrealistic ones over 50%, without looking at their significance because otherwise the trend dataset would show too few values due to the shortness of the timeseries for this analysis (less than one decade). We use the relative trends for the analysis to decouple the consideration from the average values.

2.3 Metric C: Seasonal amplitude

To determine a multi-annual mean annual cycle, the mean of all data of one calender month in all years available from the instrument is calculated for each grid cell.

In order to reduce the influence of natural variability from the statistical analysis of the climate, average values over a climatological reference period of at least 30 years (World Meteorological Organization, 2017) should be used when considering climatology according to recommendations of the WMO (World Meteorological Organization). For the observation with satellite instruments, as in this work, there is no data basis from a single instrument over such a period of time. For this reason, and

https://doi.org/10.5194/egusphere-2026-2885
Preprint. Discussion started: 12 June 2026

for simplification, a mean value, which is determined over the available period per instrument of 6 to 11 years, is used.
The amplitude of the multi-annual mean annual cycle amp is a measure for annual fluctuations and is calculated as

$$amp_{\text{seasonal}} = 0.5(x_{\max} - x_{\min}). \tag{3}$$

2.4 Metric D: Pearson correlation coefficients for the CDR of different algorithms

The Pearson correlation coefficient ρ summarizes the characteristics of a pair of datasets describing the strength and direction of the linear relationship between two variables (X and Y) (Benesty et al., 2009).

$$\rho_{X,Y} = \frac{\mathbb{E}[(X - \mu_X)(Y - \mu_Y)]}{\sigma_X \sigma_Y} \tag{4}$$

where $\mathbb{E}$ is the expectation, μ_X is the mean and σ_X is the standard deviation of X and analogue μ_Y is the mean and σ_Y is the standard deviation of Y.
As we are comparing datasets showing the same variable at the same time and place, we define datasets with a Pearson correlation coefficient larger than 0.7 as consistent in point of view of a linear correlation.

3 Examplary analysis of AOD CDR

3.1 Instruments characterization and aerosol datasets

This study analyses exemplary the Aerosol Optical Depth (AOD) at $550\,\text{nm}$ data retrieved within the C3S (Copernicus Climate Change Service, 2019) from the dual-view instruments ATSR-2 on ERS-2 (European Remote Sensing Satellite 2) (1995 - 2002), AATSR on ENVISAT (ENVironmental SATellite) (2002 - 2011) and SLSTR on Sentinel 3-A and 3-B (since 2017 and 2018, respectively). The algorithms retrieve AOD products on a $10\,\text{km}$ resolution (Level 2), which are combined into 1°x1° resolution daily and monthly products (Level 3). These monthly products are analysed in this study. In contrast to measurements with single-view instruments, the dual-view principle enables a better decoupling of the radiation contributions from the ground and the atmosphere (by approximately doubling the distance travelled by the light in the oblique view). As a result, both parts can be retrieved more accurately (Barton et al., 1989).
The instruments measure in the nadir direction and at a 55° angle in flight direction (“forward”) for ATSR-2 and AATSR and at a 55° angle against the flight direction (“rearward”) for SLSTR.
The instruments ATSR-2 and AATSR measure Top-of-atmosphere (TOA) reflectance at $550\,\text{nm}$, $665\,\text{nm}$, $865\,\text{nm}$, $1610\,\text{nm}$ and $3740\,\text{nm}$ and Brightness Temperature (BT) at $10\,850\,\text{nm}$ and $12\,000\,\text{nm}$. The SLSTR instrument has additional channels providing TOA reflectance at $1300\,\text{nm}$ and $2250\,\text{nm}$.

The data of three algorithms retrieving AOD from the data of the dual-view instruments are considered in this study. These algorithms are: ORAC (Optimal Retrieval of Aerosol and Cloud) from Oxford University (Thomas and Popp, 2024), SU from

https://doi.org/10.5194/egusphere-2026-2885
Preprint. Discussion started: 12 June 2026

Swansea University (North et al., 2024a, b) and for AATSR ADV/ASV, where ADV is ATSR dual-view (over land) and ASV is ATSR single-view (over ocean) (Kolmonen, 2024) and for SLSTR consequently SDV/SSV (Sogacheva, 2024) hereinafter summarised as FMI from the Finnish Meteorological institute. Main principles of the retrieval approaches are summarised in Table 1.

Table 1. Main characteristics of the FMI, SU and ORAC retrieval approaches following Sogacheva et al. (2020) and the versions used.

Algorithms	Principles based on	Version used	Further literature
FMI	Land: spectral constant reflectance ratio. Ocean: modelled reflectance.	ATSR-2, AATSR: v4.1; SLSTR: v2.30	(Flowerdew and Haigh, 1995; Veefkind et al., 1998; Kolmonen et al., 2016; Sogacheva et al., 2017)
SU	Iterative model inversion for continuous retrieval of AOD and fine mode fraction (FMF). Land: retrieval of bi-directional reflectance distribution factor (BRDF) parameters. Ocean: prior reflectance model.	ATSR-2, AATSR: v4.33; SLSTR: v1.12	(North et al., 1999; North, 2002; Bevan et al., 2012)
ORAC	Optimal estimation. Land: SU surface parametrisation. Ocean: sea surface reflectance model.	ATSR-2, AATSR: v4.02; SLSTR: v1.00	(Thomas et al., 2009; Sayer et al., 2010)

3.2 Results of the AOD consistency analysis

The results of the consistency analysis in the four individual metrics and the combined consistency score within two standard deviations for the three dual-view instruments are described in the following and shown in Figure 2 and Figure 3.

3.2.1 Metric A: AOD Median

When looking at the maps of median consistency (Figure 2 row 1), it can be clearly seen that ATSR-2 has a reasonable consistency of median values, especially over land, with more frequent inconsistencies over semi-arid areas and in the Southern Hemisphere (SH), over areas with high AOD over the ocean and over the Southern polar ocean. AATSR shows a similar picture with less consistency in the Southern Ocean and large areas of consistency over land with the exception of Australia, South Africa and parts of South America. SLSTR shows a clear difference - here, consistency in the median values can be mainly found between 30°N and 60°S, including over the oceans. Larger inconsistencies occur here in the range between 30°N and 60°N over both land and ocean.

https://doi.org/10.5194/egusphere-2026-2885
Preprint. Discussion started: 12 June 2026

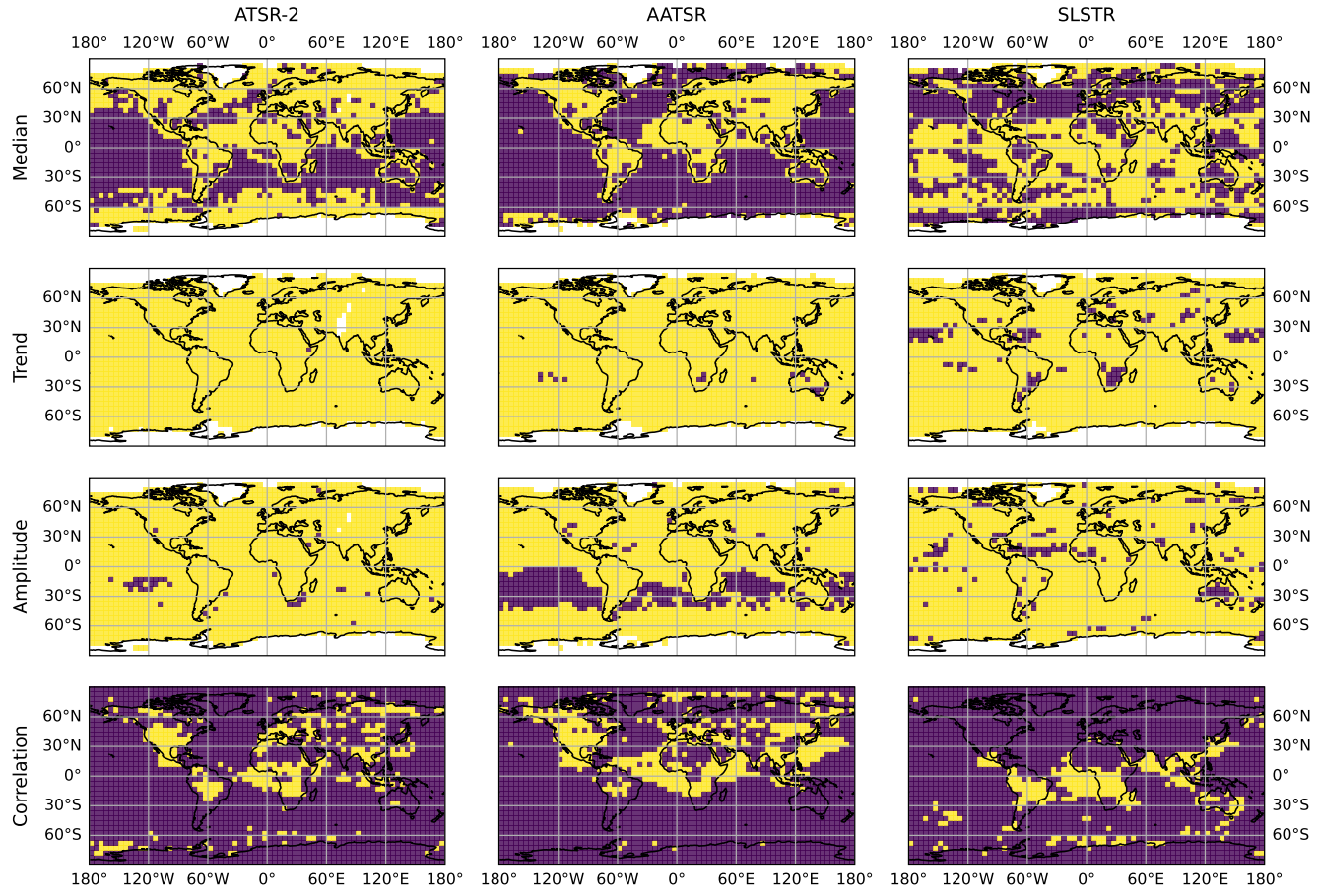

Figure 2. Consistency maps for the individual metrics (median value (row 1), trend (row 2), amplitude of the average annual cycle (row 3) and correlation coefficient (row 4) for the three instruments: ATSR-2 (left column), AATSR (middle column) and SLSTR (right column). Yellow (score = 1) means consistency in the respective metric within the required threshold, and purple (score = 0) means that there is no consistency in the 5°x5° grid box.

3.2.2 Metric B: AOD Trend

If we now look at maps of trend consistency in the AOD, globally consistent values can be seen for all three considered instruments (Figure 2 row 2). While there are no inconsistencies for ATSR-2, there are isolated inconsistencies for AATSR in the SH. These become more frequent with the SLSTR instrument and occur globally both over land (e.g. South Africa and South America) and over the ocean (e.g. in the Pacific).

https://doi.org/10.5194/egusphere-2026-2885
Preprint. Discussion started: 12 June 2026

3.2.3 Metric C: AOD annual cycle amplitude

The amplitude of the annual cycle (Figure 2 row 3) in the maps shows as largely consistent between the data sets. AATSR shows inconsistencies in the roaring forties over the Southern ocean, which only occur very sporadically in ATSR-2. For SLSTR, however, inconsistencies are more likely to be found in the Northern Hemisphere (NH) over the ocean and over the Sahara and Australia.

3.2.4 Metric D: AOD Correlation

Maps for correlation consistency (Figure 2 row 4) show consistency for ATSR-2 and AATSR mainly over land and areas over the ocean with high AOD (for example, in the Atlantic under the influence of Saharan dust and biomass burning in West Africa or in the Pacific in the area of the Asian outflow) over the NH with more consistent areas for the AATSR instrument. SLSTR, in contrast, shows a correlation between the AOD products in the SH, but also in areas over land or with high AOD over ocean.

3.2.5 Combined consistency score of the different algorithms for the three dual-view instruments

Figure 3 middle shows the map of a combined consistency score obtained as sum of the individual consistency metrics per grid cell from Figure 2 for the AATSR instrument. Major inconsistencies (consistency score of 0 or 1) can be seen mainly in the oceans in the SH. Over land and in areas above the ocean with high AOD, there is good consistency (score of 3 or 4) - with semi-arid areas showing less consistency than forested areas and higher score tending to occur in the NH than in the SH.

For ATSR-2 Figure 3 top shows a similar picture, whereby the entire ocean area, with the exception of the areas with large dust transport, show low consistency (score up to 2). Over land, over areas with high AOD over the ocean and in the polar region South of 60°S, there is mostly a consistency score of 3 or 4. Compared to AATSR, over land there are fewer areas with consistency score of 4, especially in forested areas.

Larger differences become obvious for SLSTR (Figure 3 bottom). The higher consistency shown for the other two instruments in the NH compared to the SH is reversed in SLSTR: In the NH, lower consistencies occur over land and ocean - mostly a score of 2 obtained mainly in two metrics (trend and annual cycle amplitude) and in areas with high AOD partly in three metrics. In the SH, there is mostly a consistency score of 3. High consistency (score of 4) is observed particularly in areas with a typically high AOD, like the dust belt. Across the Sahara, Australia and South Africa, all three instruments show comparatively low consistency.

3.3 Discussion of the AOD consistency analysis

Section 3.2 shows that the AOD products from three dual-view algorithms applied to similar satellite instruments are consistent over parts of the globe, but with distinct patterns. For (A)ATSR(-2) consistent areas (score of 3 or 4) are mainly over land in

https://doi.org/10.5194/egusphere-2026-2885
Preprint. Discussion started: 12 June 2026

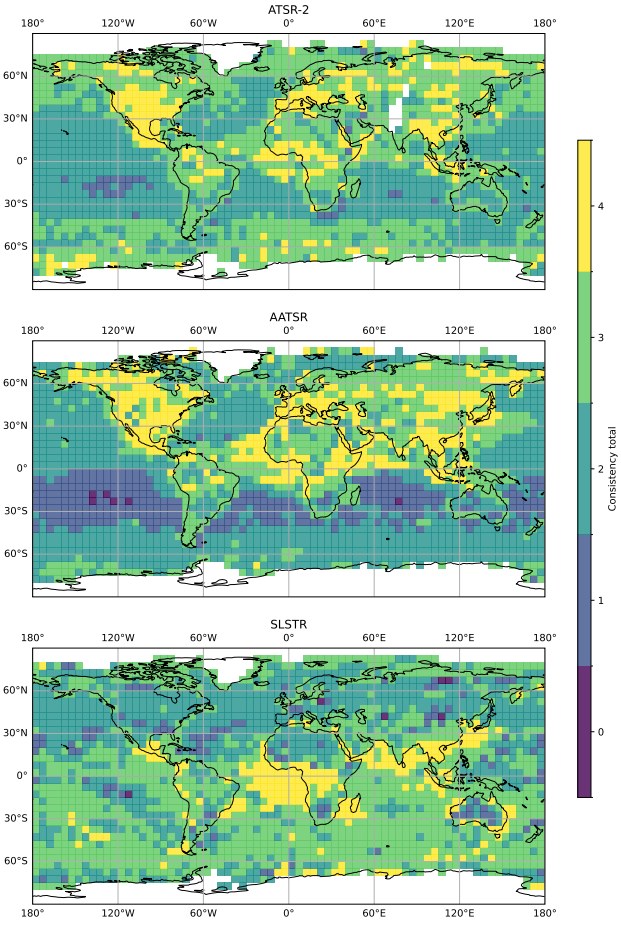

Figure 3. Maps of combined consistency scores for the three dual-view instruments: a) ATSR-2, b) AATSR and c) SLSTR

the NH, while for SLSTR over ocean in the SH. This relates clearly to the impact of the different viewing direction used for SLSTR compared for the other two instruments.

The poorer coverage and the shorter time series can explain the partially poorer consistency of ATSR-2 compared to AATSR. The largest consistency can be shown for AATSR which can be explained on the one hand since the longest time series so far is available from this instrument and on the other hand by the fact that most development and harmonisation work so far has been spent on this sensor. The striking differences in consistency between (A)ATSR(-2) and SLSTR, in particular the reversal from higher consistency in the NH for (A)ATSR(-2) to larger consistency in the SH for SLSTR, can be attributed to the changed oblique viewing direction, from forwards to backwards. As described in (Pearson et al., 2024), the change in viewing direction leads to larger uncertainties due to a higher fraction of observations in the adverse backward scattering direction.

https://doi.org/10.5194/egusphere-2026-2885
Preprint. Discussion started: 12 June 2026

The lower observed consistency over ocean could be due to the generally lower values and thus more difficult determination of the AOD. Furthermore, the low number of ground measurements over the ocean limits achievable quality and harmonisation of retrieval results during the development process. Over deserts, such as the Sahara, the brighter soil makes aerosol retrieval from solar channels more difficult, which could explain the lower consistencies here. Over desert areas in the SH, in South Africa, South America and Australia, this is made even more difficult by the different composition of the desert soil. The largest coverage by ground monitoring stations in Europe and North America and the increased research interest in algorithm development in these regions, in addition to better visibility over dark, for example vegetated ground, may have led to the highest consistency of the data obtained in these areas.

A comparison to ground measuring stations, like AERONET (AErosol RObotic NETwork) (Holben et al., 1998) or MAN (Maritime Aerosol Network) (Smirnov et al., 2009), is still necessary to evaluate the absolute accuracy of the algorithms.

As highlighted in (Sogacheva et al., 2020), no single algorithm consistently outperforms all others in every situation. An uncertainty-weighted median ensemble as provided in addition by C3S aims to combine the strengths and suppress the weaknesses of the individual algorithms Popp (2024).

4 Conclusions

As shown in the exemplary AOD consistency analysis the consistency approach works good in regions with stable conditions and not much noise in the data. It is able to discriminate regions with consistent datasets and regions with differences in the datasets. This can help to differentiate between regions where all datasets can be trusted and regions where a careful look is needed when choosing the right dataset for an individual application.

The method to analyse the consistency has certain limitations, for example in areas with spatial data gaps or a lot of noise in the data, such as in polar regions and partly over other bright surface areas like deserts. Data with large noise or large variances between neighbouring 1°x1° grid cells have a large standard deviation, making it easier to erroneously label data as consistent in these areas. The high consistency that can sometimes be observed over polar regions could be explained by these large fluctuations due to difficulties in the retrieval for example by the low position of the sun or by seasonal data gaps. However, in regions with less noisy data and more stable retrieval conditions this consistency analysis works well.

The choice of metrics and thresholds for each of them can strongly influence the results. The method can be adjusted with customized threshold values for the metrics to filter out the appropriate areas depending on a concrete use case and its quantitative requirements. It can also be useful to only consider individual metrics which are relevant for a particular application. For example, if trends in different regions are to be compared, only the trend metric could be considered.

https://doi.org/10.5194/egusphere-2026-2885
Preprint. Discussion started: 12 June 2026

Overall, this study shows that its approach can help users to quickly and easily understand the consistency for a specific study purpose and area and thus to identify areas in which the data can be used more efficiently and areas where the datasets should be handled with care. Depending on the use case it can make sense to look at the metrics individually.

5 Data availability

The aerosol data from dual-view sensors (A)ATSR(-2) and SLSTR which are analysed in this paper can be accessed from the Copernicus Climate Change Service in July 2024: Copernicus Climate Change Service, Climate Data Store, (2019): Aerosol properties gridded data from 1995 to present derived from satellite observation. Copernicus Climate Change Service (C3S) Climate Data Store (CDS) under data DOI: 10.24381/cds.239d815c Copernicus Climate Change Service (2019). The algorithms and versions used can be taken from Table 1.

Author contributions. All authors conceived the research and significantly contributed to the scientific discussions. US and DD developed the method used with support of TP. US developed the code for the study and prepared the manuscript with valuable input from TP and DD. TP introduced the idea of analysing the consistency of the data sets used.

Competing interests. The authors declare no conflicts of interest.

Acknowledgements. The aerosol data from dual-view sensors (A)ATSR(-2) and SLSTR which are analysed in this paper were obtained from the Copernicus Climate Change Service in July 2024: Copernicus Climate Change Service, Climate Data Store, (2019): Aerosol properties gridded data from 1995 to present derived from satellite observation. Copernicus Climate Change Service (C3S) Climate Data Store (CDS). DOI: 10.24381/cds.239d815c (Accessed on 20-MAR-2026). Neither the European Commission nor ECMWF is responsible for any use that may be made of the Copernicus information or data it contains. Furthermore, we want to thank the responsible providers of the (A)ATSR(-2) and SLSTR aerosol data which we analysed: Larisa Sogacheva at FMI, Gareth Thomas at RAL and Peter North at Swansea University. We also want to thank Larisa Sogacheva for her input to improve the metrics and the manuscript.

https://doi.org/10.5194/egusphere-2026-2885
Preprint. Discussion started: 12 June 2026

References

Allen, M., Dube, O., Solecki, W., Aragón-Durand, F., Cramer, W., Humphreys, S., Kainuma, M., Kala, J., Mahowald, N., Mulugetta, Y., Perez, R., M.Wairiu, and Zickfeld, K.: Global Warming of 1.5°C. An IPCC Special Report on the impacts of global warming of 1.5°C above pre-industrial levels and related global greenhouse gas emission pathways, in the context of strengthening the global response to the threat of climate change, sustainable development, and efforts to eradicate poverty, chap. Framing and Context, Cambridge University Press, 2018.

Arias, P., Bellouin, N., Coppola, E., Jones, R., Krinner, G., Marotzke, J., Naik, V., Palmer, M., Plattner, G.-K., Rogelj, J., Rojas, M., Sillmann, J., Storelvmo, T., Thorne, P., Trewin, B., Rao, K. A., Adhikary, B., Allan, R., Armour, K., Bala, G., Barimalala, R., Berger, S., Canadell, J., Cassou, C., Cherchi, A., Collins, W., Collins, W., Connors, S., Corti, S., Cruz, F., Dentener, F., Dereczynski, C., Luca, A. D., Niang, A. D., Doblas-Reyes, F., Dosio, A., Douville, H., Engelbrecht, F., Eyring, V., Fischer, E., Forster, P., Fox-Kemper, B., Fuglestvedt, J., Fyfe, J., Gillett, N., Goldfarb, L., Gorodetskaya, I., Gutierrez, J., Hamdi, R., Hawkins, E., Hewitt, H., Hope, P., Islam, A., Jones, C., Kaufman, D., Kopp, R., Kosaka, Y., Kossin, J., Krakovska, S., Lee, J.-Y., Li, J., Mauritsen, T., Maycock, T., Meinshausen, M., Min, S.-K., Monteiro, P., Ngo-Duc, T., Otto, F., Pinto, I., Pirani, A., Raghavan, K., Ranasinghe, R., Ruane, A., Ruiz, L., Sallée, J.-B., Samset, B., Sathyendranath, S., Seneviratne, S., Sörensson, A., Szopa, S., Takayabu, I., Tréguier, A.-M., van den Hurk, B., Vautard, R., von Schuckmann, K., Zaehle, S., Zhang, X., and Zickfeld, K.: Technical Summary in Climate Change 2021 – The Physical Science Basis: Working Group I Contribution to the Sixth Assessment Report of the Intergovernmental Panel on Climate Change, pp. 35–144, Cambridge University Press, https://doi.org/10.1017/9781009157896.002, 2021.

Barton, I. J., Zavody, A. M., O'Brien, D. M., Cutten, D. R., Saunders, R. W., and Llewellyn-Jones, D. T.: Theoretical algorithms for satellite-derived sea surface temperatures, Journal of Geophysical Research: Atmospheres, 94, 3365–3375, https://doi.org/10.1029/jd094id03p03365, 1989.

Benesty, J., Chen, J., Huang, Y., and Cohen, I.: Pearson Correlation Coefficient, pp. 1–4, Springer Berlin Heidelberg, Berlin, Heidelberg, ISBN 978-3-642-00296-0, https://doi.org/10.1007/978-3-642-00296-0_5, 2009.

Bevan, S. L., North, P. R., Los, S. O., and Grey, W. M.: A global dataset of atmospheric aerosol optical depth and surface reflectance from AATSR, Remote Sensing of Environment, 116, 199–210, https://doi.org/10.1016/j.rse.2011.05.024, advanced Along Track Scanning Radiometer (AATSR) Special Issue, 2012.

Copernicus Climate Change Service: Aerosol properties gridded data from 1995 to present derived from satellite observations, https://doi.org/10.24381/cds.239d815c, (Accessed on 20-08-2024), 2019.

de Leeuw, G., Holzer-Popp, T., Bevan, S., Davies, W. H., Descloitres, J., Grainger, R. G., Griesfeller, J., Heckel, A., Kinne, S., Klüser, L., Kolmonen, P., Litvinov, P., Martynenko, D., North, P., Ovigneur, B., Pascal, N., Poulsen, C., Ramon, D., Schulz, M., Siddans, R., Sogacheva, L., Tanré, D., Thomas, G. E., Virtanen, T. H., von Hoyningen Huene, W., Vountas, M., and Pinnock, S.: Evaluation of seven European aerosol optical depth retrieval algorithms for climate analysis, Remote Sensing of Environment, 162, 295–315, https://doi.org/10.1016/j.rse.2013.04.023, 2015.

Flowerdew, R. J. and Haigh, J. D.: An approximation to improve accuracy in the derivation of surface reflectances from multi-look satellite radiometers, Geophysical Research Letters, 22, 1693–1696, https://doi.org/10.1029/95GL01662, 1995.

Hirsch, R. M., Slack, J. R., and Smith, R. A.: Techniques of trend analysis for monthly water quality data, Water Resources Research, 18, 107–121, https://doi.org/10.1029/WR018i001p00107, 1982.

https://doi.org/10.5194/egusphere-2026-2885
Preprint. Discussion started: 12 June 2026

Holben, B., Eck, T., Slutsker, I., Tanré, D., Buis, J., Setzer, A., Vermote, E., Reagan, J., Kaufman, Y., Nakajima, T., Lavenu, F., Jankowiak, I., and Smirnov, A.: AERONET—A Federated Instrument Network and Data Archive for Aerosol Characterization, Remote Sensing of Environment, 66, 1–16, https://doi.org/10.1016/s0034-4257(98)00031-5, 1998.

Hollmann, R., Merchant, C. J., Saunders, R., Downy, C., Buchwitz, M., Cazenave, A., Chuvieco, E., Defourny, P., de Leeuw, G., Forsberg, R., Holzer-Popp, T., Paul, F., Sandven, S., Sathyendranath, S., van Roozendael, M., and Wagner, W.: The ESA Climate Change Initiative: Satellite Data Records for Essential Climate Variables, Bulletin of the American Meteorological Society, 94, 1541–1552, https://doi.org/10.1175/BAMS-D-11-00254.1, 2013.

Hussain, M. and Mahmud, I.: pyMannKendall: a python package for non parametric Mann Kendall family of trend tests., Journal of Open Source Software, 4, 1556, https://doi.org/10.21105/joss.01556, 2019.

Kendall, M. G.: Rank correlation methods, Griffin London, fourth edn., 1970.

Kokhanovsky, A. A. and Leeuw, G.: Satellite Aerosol Remote Sensing over Land, Springer Berlin Heidelberg, ISBN 9783540693970, https://doi.org/10.1007/978-3-540-69397-0, 2009.

Kolmonen, P.: C3S2_312a_Lot2 Algorithm Theoretical Basis Document, Annex A1: ADV/ASV, Tech. rep., E.U. Copernicus Climate Change Service, https://datastore.copernicus-climate.eu/documents/satellite-aerosol-properties/C3S2_312a_Lot2_FDDP-AER/C3S2_312a_Lot2_D-WP2-FDDP-AER_202311_ATBD_AER_v2.0_final2.pdf, 2024.

Kolmonen, P., Sogacheva, L., Virtanen, T. H., de Leeuw, G., and Kulmala, M.: The ADV/ASV AATSR aerosol retrieval algorithm: current status and presentation of a full-mission AOD dataset, International Journal of Digital Earth, 9, 545–561, https://doi.org/10.1080/17538947.2015.1111450, 2016.

Li, J., Carlson, B. E., Dubovik, O., and Lacis, A. A.: Recent trends in aerosol optical properties derived from AERONET measurements, Atmospheric Chemistry and Physics, 14, 12 271–12 289, https://doi.org/10.5194/acp-14-12271-2014, 2014.

Mann, H. B.: Nonparametric Tests Against Trend, Econometrica, 13, 245, https://doi.org/10.2307/1907187, 1945.

North, P., Briggs, S., Plummer, S., and Settle, J.: Retrieval of land surface bidirectional reflectance and aerosol opacity from ATSR-2 multi-angle imagery, IEEE Transactions on Geoscience and Remote Sensing, 37, 526–537, https://doi.org/10.1109/36.739106, 1999.

North, P., Heckel, A., Pearson, K., and Popp, T.: C3S2_312a_Lot2 Algorithm Theoretical Basis Document, Annex C1: SU ATSR, Tech. rep., E.U. Copernicus Climate Change Service, https://datastore.copernicus-climate.eu/documents/satellite-aerosol-properties/C3S2_312a_Lot2_FDDP-AER/C3S2_312a_Lot2_D-WP2-FDDP-AER_202311_ATBD_AER_Annex_C1_SU_ATSR_v2.0_final.pdf, 2024a.

North, P., Heckel, A., Pearson, K., and Popp, T.: C3S2_312a_Lot2 Algorithm Theoretical Basis Document, Annex C2: SU SLSTR, Tech. rep., E.U. Copernicus Climate Change Service, https://datastore.copernicus-climate.eu/documents/satellite-aerosol-properties/C3S2_312a_Lot2_FDDP-AER/C3S2_312a_Lot2_D-WP2-FDDP-AER_202311_ATBD_AER_v2.0_final2.pdf, 2024b.

North, P. R. J.: Estimation of aerosol opacity and land surface bidirectional reflectance from ATSR-2 dual-angle imagery: Operational method and validation, Journal of Geophysical Research: Atmospheres, 107, AAC 4–1–AAC 4–10, https://doi.org/10.1029/2000JD000207, 2002.

Pearson, K., North, P., Heckel, A., Hornero, A., Kinne, S., Popp, T., Sogacheva, L., and Griesfeller, J.: Atmospheric aerosol measurements from the ATSR-SLSTR series of dual-view satellite instruments 1995-2012 and 2016-2022, submitted to Nature Scientific Data, 2024.

Popp, T.: C3S2_312a_Lot2 Algorithm Theoretical Basis Document, main, Tech. rep., E.U. Copernicus Climate Change Service, https://datastore.copernicus-climate.eu/documents/satellite-aerosol-properties/C3S2_312a_Lot2_FDDP-AER/C3S2_312a_Lot2_D-WP2-FDDP-AER_202311_ATBD_AER_v2.0_final2.pdf, 2024.

Popp, T., de Leeuw, G., Bingen, C., Brühl, C., Capelle, V., Chedin, A., Clarisse, L., Dubovik, O., Grainger, R., Griesfeller, J., Heckel, A., Kinne, S., Klüser, L., Kosmale, M., Kolmonen, P., Lelli, L., Litvinov, P., Mei, L., North, P., Pinnock, S., Povey, A., Robert, C., Schulz, M.,

https://doi.org/10.5194/egusphere-2026-2885
Preprint. Discussion started: 12 June 2026

Sogacheva, L., Stebel, K., Zweers, D. S., Thomas, G., Tilstra, L., Vandenbussche, S., Veefkind, P., Vountas, M., and Xue, Y.: Development, Production and Evaluation of Aerosol Climate Data Records from European Satellite Observations (Aerosol_cci), Remote Sensing, 8, 421, https://doi.org/10.3390/rs8050421, 2016.

Popp, T., Hegglin, M. I., Hollmann, R., Ardhuin, F., Bartsch, A., Bastos, A., Bennett, V., Boutin, J., Brockmann, C., Buchwitz, M., Chuvieco, E., Ciais, P., Dorigo, W., Ghent, D., Jones, R., Lavergne, T., Merchant, C. J., Meyssignac, B., Paul, F., Quegan, S., Sathyendranath, S., Scanlon, T., Schröder, M., Simis, S. G. H., and Willén, U.: Consistency of Satellite Climate Data Records for Earth System Monitoring, Bulletin of the American Meteorological Society, 101, E1948–E1971, https://doi.org/10.1175/BAMS-D-19-0127.1, 2020.

Sayer, A. M., Thomas, G. E., and Grainger, R. G.: A sea surface reflectance model for (A)ATSR, and application to aerosol retrievals, Atmospheric Measurement Techniques, 3, 813–838, https://doi.org/10.5194/amt-3-813-2010, 2010.

Smirnov, A., Holben, B. N., Slutsker, I., Giles, D. M., McClain, C. R., Eck, T. F., Sakerin, S. M., Macke, A., Croot, P., Zibordi, G., Quinn, P. K., Sciare, J., Kinne, S., Harvey, M., Smyth, T. J., Piketh, S., Zielinski, T., Proshutinsky, A., Goes, J. I., Nelson, N. B., Larouche, P., Radionov, V. F., Goloub, P., Krishna Moorthy, K., Matarrese, R., Robertson, E. J., and Jourdin, F.: Maritime Aerosol Network as a component of Aerosol Robotic Network, Journal of Geophysical Research: Atmospheres, 114, https://doi.org/10.1029/2008jd011257, 2009.

Sogacheva, L.: C3S2_312a_Lot2 Algorithm Theoretical Basis Document, Annex A2: SDV/SSV, Tech. rep., E.U. Copernicus Climate Change Service, https://datastore.copernicus-climate.eu/documents/satellite-aerosol-properties/C3S2_312a_Lot2_FDDP-AER/C3S2_312a_Lot2_D-WP2-FDDP-AER_202311_ATBD_AER_Annex_A2_SDV_v4.1_final.pdf, 2024.

Sogacheva, L., Kolmonen, P., Virtanen, T. H., Rodriguez, E., Saponaro, G., and de Leeuw, G.: Post-processing to remove residual clouds from aerosol optical depth retrieved using the Advanced Along Track Scanning Radiometer, Atmospheric Measurement Techniques, 10, 491–505, https://doi.org/10.5194/amt-10-491-2017, 2017.

Sogacheva, L., Popp, T., Sayer, A. M., Dubovik, O., Garay, M. J., Heckel, A., Hsu, N. C., Jethva, H., Kahn, R. A., Kolmonen, P., Kosmale, M., de Leeuw, G., Levy, R. C., Litvinov, P., Lyapustin, A., North, P., Torres, O., and Arola, A.: Merging regional and global aerosol optical depth records from major available satellite products, Atmospheric Chemistry and Physics, 20, 2031–2056, https://doi.org/10.5194/acp-20-2031-2020, 2020.

Thomas, G. and Popp, T.: C3S2_312a_Lot2 Algorithm Theoretical Basis Document, Annex B: ORAC, Tech. rep., E.U. Copernicus Climate Change Service, https://datastore.copernicus-climate.eu/documents/satellite-aerosol-properties/C3S2_312a_Lot2_FDDP-AER/C3S2_312a_Lot2_D-WP2-FDDP-AER_202311_ATBD_AER_Annex_B_ORAC_v2.0_final2.pdf, 2024.

Thomas, G. E., Carboni, E., Sayer, A. M., Poulsen, C. A., Siddans, R., and Grainger, R. G.: Oxford-RAL Aerosol and Cloud (ORAC): aerosol retrievals from satellite radiometers, pp. 193–225, Springer Berlin Heidelberg, Berlin, Heidelberg, ISBN 978-3-540-69397-0, https://doi.org/10.1007/978-3-540-69397-0_7, 2009.

Veefkind, J. P., de Leeuw, G., and Durkee, P. A.: Retrieval of aerosol optical depth over land using two-angle view satellite radiometry during TARFOX, Geophysical Research Letters, 25, 3135–3138, https://doi.org/10.1029/98GL02264, 1998.

World Meteorological Organization: WMO Guidelines on the Calculation of Climate Normals, no. 1203 in WMO, ISBN 978-92-63-11203-3, 2017.